Received: 1 October 2021 | Revised: 9 December 2021 | Accepted: 10 December 2021

DOI: 10.1111/mmi.14863

RESEARCH ARTICLE

WILEY

EPEC-induced activation of the Ca^{2+} transporter TRPV2 leads to pyroptotic cell death

Qiyun Zhong [1] | Sharanya Chatterjee [1] | Jyoti S. Choudhary [2] | Gad Frankel [1]

[1]Centre for Molecular Bacteriology and Infection, Department of Life Sciences, Imperial College, London, UK

[2]Functional Proteomics Group, Chester Beatty Laboratories, The Institute of Cancer Research, London, UK

Correspondence
Gad Frankel, Centre for Molecular Bacteriology and Infection, Department of Life Sciences, Imperial College, London, UK.
Email: g.frankel@imperial.ac.uk

Jyoti S. Choudhary, Functional Proteomics Group, Chester Beatty Laboratories, The Institute of Cancer Research, London, UK.
Email: jyoti.choudhary@icr.ac.uk

Funding information
Wellcome Trust, Grant/Award Number: 107057/Z/15/Z; Medical Research Council

Abstract

The enteropathogenic *Escherichia coli* (EPEC) type III secretion system effector Tir, which mediates intimate bacterial attachment to epithelial cells, also triggers Ca^{2+} influx followed by LPS entry and caspase-4-dependent pyroptosis, which could be antagonized by the effector NleF. Here we reveal the mechanism by which EPEC induces Ca^{2+} influx. We show that in the intestinal epithelial cell line SNU-C5, Tir activates the mechano/osmosensitive cation channel TRPV2 which triggers extracellular Ca^{2+} influx. Tir-induced Ca^{2+} influx could be blocked by siRNA silencing of TRPV2, pre-treatment with the TRPV2 inhibitor SET2 or by growing cells in low osmolality medium. Pharmacological activation of TRPV2 in the absence of Tir failed to initiate caspase-4-dependent cell death, confirming the necessity of Tir. Consistent with the model implicating activation on translocation of TRPV2 from the ER to plasma membrane, inhibition of protein trafficking by either brefeldin A or the effector NleA prevented TRPV2 activation and cell death. While infection with EPECΔ*nleA* triggered pyroptotic cell death, this could be prevented by NleF. Taken together this study shows that while integration of Tir into the plasma membrane activates TRPV2, EPEC uses NleA to inhibit TRPV2 trafficking and NleF to inhibit caspase-4 and pyroptosis.

KEYWORDS
Caspases, enteropathogenic *Escherichia coli*, protein transport, pyroptosis, transient receptor potential channels, type III secretion systems

1 | INTRODUCTION

Enteropathogenic *Escherichia coli* (EPEC) is an extracellular human diarrheal pathogen mainly in children under 5 years old in low-income regions (Chen & Frankel, 2005). EPEC E2348/69 uses the type III secretion system (T3SS), a syringe-like molecular machine, to translocate 21 virulence factors called effectors into the host cells which subvert multiple signaling pathways such as cytoskeleton dynamics, tight junctions, inflammation, vesicle trafficking, and cell survival (Garmendia et al., 2005; Shenoy et al., 2018). EPEC colonization of intestinal epithelial cells (IECs) is dependent on injection of the translocated intimin receptor (Tir), which inserts into host plasma membrane in a hairpin loop topology and forms a receptor for the *eae*-encoded bacterial outer membrane protein intimin (Frankel et al., 2001; Kenny et al., 1997). Clustering of Tir by intimin leads to phosphorylation of the tyrosine residues Y454 (Brady et al., 2007; Campellone & Leong, 2005; Sason et al., 2009; Vingadassalom et al., 2009; Weiss et al., 2009) and Y474 (Campellone et al., 2004; Gruenheid et al., 2001; Rohatgi et al., 2001) by host tyrosine kinases followed by recruitment of adaptor proteins and actin polymerization

(Bommarius et al., 2007; Brady et al., 2007; Hayward et al., 2009; Kalman et al., 1999; Phillips et al., 2004; Swimm et al., 2004).

Apart from its involvement in bacterial adhesion, accumulating evidence suggests that integration of Tir into the plasma membrane induces activation of pyroptosis, a lytic and pro-inflammatory cell death (Goddard et al., 2019; Zhong et al., 2020). Pyroptosis can be activated by pathogen/damage-associated molecular patterns (PAMPs/DAMPs) via the canonical inflammasome, consisting of three components: (a) a sensor (NLR-family proteins, pyrin or AIM-2), (b) the adaptor Asc, (c) and the executor caspase-1; pyroptosis could also be activated by the non-canonical inflammasome, consisting of the lipopolysaccharide (LPS)-activated caspase-4 or its homolog caspase-5 (Kayagaki et al., 2013; Broz & Dixit, 2016; Vande Walle & Lamkanfi, 2016; Sanchez-Garrido et al., 2020), which may require the LPS-binding protein GBP1 to form a caspase-activation platform (Fisch et al., 2019; Santos et al., 2020). Active caspase-1, -4, and -5 cleave gasdermin-D (GSDMD), freeing its N-terminus domain that forms pores in the plasma membrane, which lead to cellular rupture and the release of intracellular contents (Kayagaki et al., 2015; Shi et al., 2015).

Intimin-mediated Tir clustering and actin polymerization in EPEC-infected macrophage lead to activation of caspase-4 and processing of GSDMD, which subsequently activates the canonical NLRP3-Asc-caspase-1 inflammasome (Goddard et al., 2019). Using EPEC wild type (WT), the EPEC-1 derivative, which expresses intimin, the T3SS and Tir as the sole effector and EPEC-0, which expresses intimin and the T3SS but none of the effectors, we showed that intimin-induced Tir clustering in the IEC model cell line SNU-C5 induces Ca^{2+} and LPS internalization which leads to caspase-4-mediated pyroptosis (Zhong et al., 2020). Cell death, as measured by propidium iodide (PI) uptake, was first seen at 2 hr post-infection and plateaued before 8 hr (Zhong et al., 2020). Tir-induced cell death in SNU-C5 cells was enhanced by pre-treatment with ATP or priming with IFNγ which promotes Ca^{2+}-influx or expression of caspase-4 and GSDMD, respectively. In contrast, cell death can be blocked by co-expression in EPEC-1 of the caspase-4-inhibiting effector NleF, silencing of caspase-4 or GSDMD or chelation of extracellular Ca^{2+} (Zhong et al., 2020).

The route of Ca^{2+} entry following EPEC-1 infection had not been elucidated. Tir-membrane insertion induces localized membrane disruptions (Lin et al., 2011), which could potentially activate mechanosensitive ion channels, such as the TRP family (Liu & Montell, 2015; Startek et al., 2019). Using whole-cell proteomics, we have recently shown that infection with EPEC-1 induces increased abundance of TRPV2 (Zhong et al., 2020). TRPV2 is a non-selective cation channel with a higher affinity to Ca^{2+} conductance compared to other ions and can be opened by various stimuli, including heat over 52°C, mechanical stretching (e.g., via osmotic stress), and cannabinoids (Caterina et al., 1999; Muraki et al., 2003; Petrocellis et al., 2011; Zanou et al., 2015). It is predominantly located in intracellular membranes, particularly the ER, in unstimulated cells. However, trafficking of TRPV2 to plasma membrane, preceding TRPV2 channel activation, can be induced by mechanical stress or growth factor stimulation (Kanzaki et al., 1999; Monet et al., 2009; Nagasawa & Kojima, 2015; Nagasawa et al., 2007; Reichhart et al., 2015). In this study, we investigated the role of TRPV2 in Tir-induced Ca^{2+} influx and pyroptosis.

2 | RESULTS

2.1 | TRPV2 contributes to Tir-induced cell death in SNU-C5 cells

We have recently shown that EPEC triggers caspase-4- and GSDMD-dependent pyroptotic cell death in SNU-C5 cells; the magnitude of cell death was amplified by pre-treatment with IFNγ, as it increases expression of caspase-4 and GSDMD (Zhong et al., 2020). EPEC-1-, but not EPEC-0, triggers activation of caspase-4 following clustering of Tir by intimin in the plasma membrane (Figure 1a). As this leads to membrane curvature (Lin et al., 2011), we hypothesized that Tir clustering creates membrane stress which could activate mechanosensitive Ca^{2+}-channels, leading to Ca^{2+}-influx required for LPS entry that subsequently activates caspase-4. We have recently reported that following EPEC-1 infection of SNU-C5 cells the protein abundance of the mechanosensitive cation channel TRPV2, which has a preference for Ca^{2+}, has increased (Zhong et al., 2020). Accordingly, we investigated if TRPV2 plays a role in EPEC-induced pyroptosis in SNU-C5 cells.

First, we used siRNA silencing to investigate the involvement of TRPV2 in EPEC-1 induced cell death. In our previous study, we have shown that EPEC-1 infection induces Ca^{2+} influx after around 20 min post-infection, followed by detectable LPS entry at 2 hr post-infection, while cell death peaks at 8 hr post-infection (Zhong et al., 2020). TRPV2 silencing by siRNA was confirmed by qRT-PCR (Figure 1b). Knock-down of TRPV2 reduced the Ca^{2+} influx and partially inhibited cell death at 20 min and 8 hr post-EPEC-1 infection of SNU-C5 cells, respectively (Figure 1c,d and Figure S1). Importantly, caspase-4 was not cleaved in EPEC-1-infected TRPV2-silenced SNU-C5 cells, demonstrating that TRPV2 activation lies upstream of caspase-4 activation (Figure 1e). Moreover, pre-treatment with SET2, an inhibitor selective for TRPV2-mediated Ca^{2+} conductance (Chai et al., 2019), also reduced Ca^{2+} influx and EPEC-1-induced cell death (Figure 1f,g), implicating the channel activity of TRPV2. A combination of SET2 and YVAD, which inhibit TRPV2 and caspase-4, respectively, did not further reduce Tir-induced cell death compared to YVAD treatment alone, confirming that TRPV2 and caspase-4 activation are involved in the same cell death pathway (Figure 1g and Figure S1). However, SET2 did not block cell death to the same magnitude as extracellular Ca^{2+} chelation by EGTA, which was higher than cell death seen following infection with EPEC-0 (Figure 1g and Figure S1), suggesting the involvement of additional Ca^{2+} influx routes.

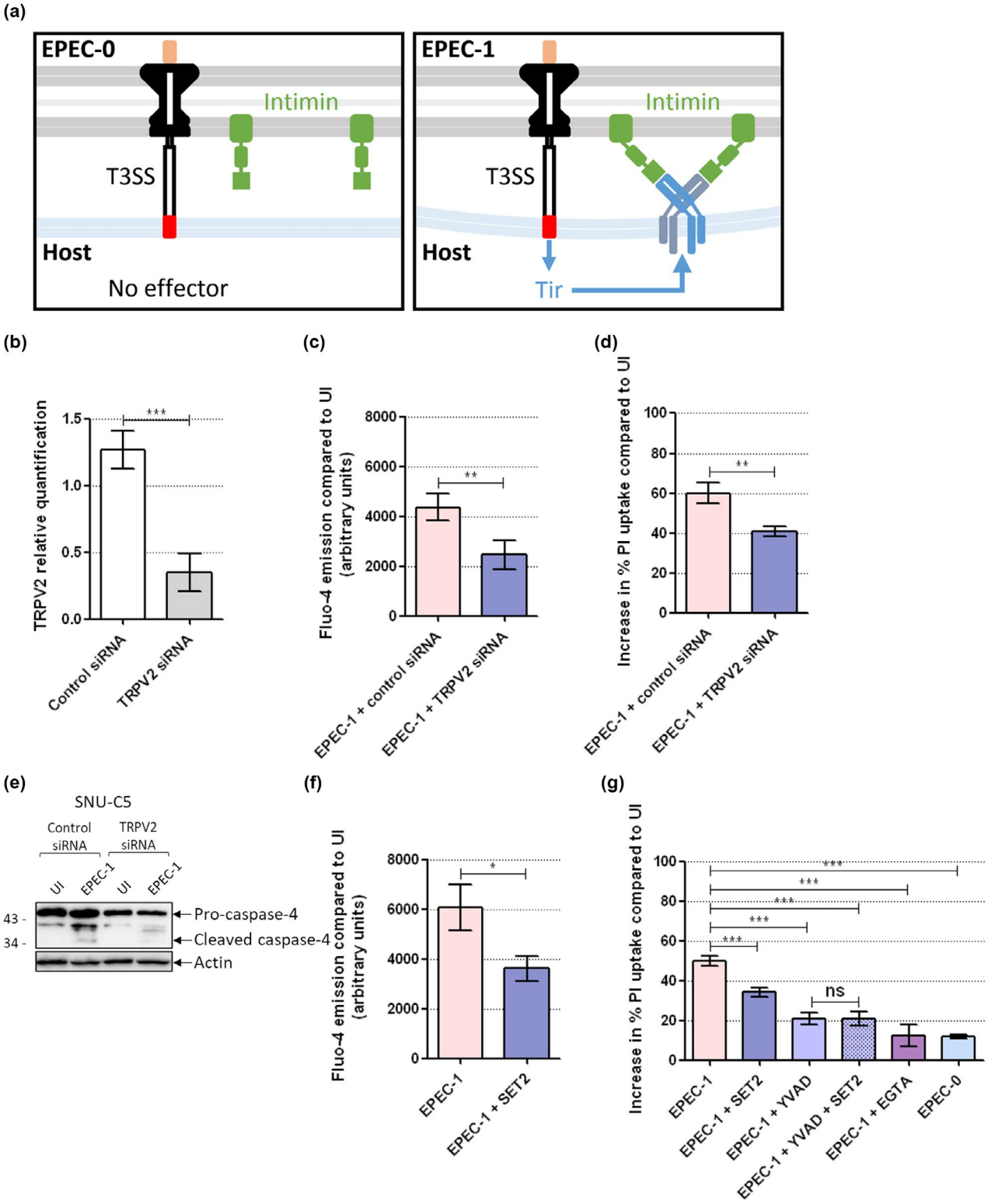

2.2 | Lowering osmolality protects cells from EPEC-1-induced cell death

Activation of TRPV2 can be achieved via membrane pressure, for example changing growth medium osmolality (Muraki et al., 2003; Zanou et al., 2015). As integration of Tir into the plasma membrane causes local distortion and membrane stress (Lin et al., 2011), we hypothesized that TRPV2 activation can be regulated by modulation of osmolality. To this end we used growth media with different osmolality, adjusted by sorbitol, to reverse or promote any potential membrane disruption induced by Tir membrane integration. Incubating SNU-C5 cells in hypertonic medium (~360 mOs/kg) did not affect EPEC-1-induced Ca^{2+} influx and cell death (Figure 2a,b). In contrast, incubation in hypotonic medium (~100 mOs/kg) significantly

FIGURE 1 TRPV2 inhibition and silencing reduce Tir-induced Ca^{2+} influx and pyroptosis. (a) Schematics of EPEC-0 and EPEC-1 interaction with epithelial cells. (b) qRT-PCR of TRPV2 mRNA from RNA extracts of SNU-C5 cells treated by control or TRPV2 siRNA for 3 days. Data were normalized to the relative quantification of TRPV2 in control siRNA-treated cells from the first biological repeat. Means ± *SEM* from $n = 3$ independent biological repeats are shown. (c) Fluo-4 assay at 20 min after EPEC-1 infection of control or TRPV2-silenced SNU-C5 cells. UI, uninfected. Means ± *SEM* from $n = 6$ independent biological repeats are shown. (d) PI uptake at 8 hr after EPEC-1 infection of control or TRPV2-silenced SNU-C5 cells. Means ± *SEM* from $n = 6$ independent biological repeats are shown. (e) Caspase-4 Western blot of combined lysates and supernatants from EPEC-1-infected control or TRPV2-silenced SNU-C5 cells. Shown is a representative blot from $n = 3$ independent biological repeats are shown. (f) Fluo-4 assay at 20 min after EPEC-1 infection of SNU-C5 cells with or without SET2 pre-treatment. Means ± *SEM* from $n = 6$ independent biological repeats are shown. (g) PI uptake at 8 hr after EPEC-1 infection of SNU-C5 cells with or without SET2, YVAD, YVAD + SET2, or EGTA pre-treatment. PI uptake of EPEC-0 infection is included as a negative control. Means ± *SEM* from $n = 10$ (SET2) and 3 (EGTA, YVAD, YVAD + SET2, and EPEC-0) independent biological repeats are shown. Statistical significance was determined using 2-tailed *t* test (b–d, f) or 1-way ANOVA with Tukey post-test (g). $^{*}p \leq .05$; $^{**}p \leq .01$; $^{***}p \leq .001$; ns, non-significant

reduced EPEC-1-induced Ca^{2+} influx and cell death (Figure 2c,d); the hypotonic medium did not affect EPEC-1-induced actin polymerization (Figure 2e) or infection outcomes with the negative control EPEC-0 (Figure 2d). Importantly, lowering osmolality did not further reduce Ca^{2+} influx in TRPV2-silenced cells, suggesting that the inhibitory effect of hypotonicity acts through TRPV2 (Figure 2c).

2.3 | Tir-induced activation of TRPV2 specifically induces caspase-4 pyroptosis

We have recently shown that Ca^{2+} influx leads to LPS internalization and activation of caspase-4 (Zhong et al., 2020). In order to investigate whether direct activation of TRPV2 could substitute Tir-induced activation during EPEC-1 infection, we treated SNU-C5 cells with the TRPV2 agonist cannabidiol (CBD) with or without extracellular LPS. Fluo-4 assay confirmed that CBD induced Ca^{2+} influx, which could be inhibited by SET2 (Figure 3a). Moreover, CBD treatment alone induced PI-uptake, which was inhibited by SET2 or TRPV2 silencing (Figure 3b,c). However, the addition of LPS to CBD-treated cells did not enhance PI uptake (Figure 3b). The pan-caspase inhibitor zVAD, which inhibits pyroptotic as well as apoptotic caspases, partially inhibited CBD-induced cell death (Figure 3b). However, specific silencing of caspase-4 by siRNA could not reduce CBD-induced cell death (Figure 3c). As caspase-4 is the only pyroptotic caspase expressed in SNU-C5 (Roumeliotis et al., 2017), CBD-induced cell death is likely dependent on the traditionally apoptotic caspases. Therefore, while activation of TRPV2 alone induces Ca^{2+} influx and cell death, Tir-induced activation of TRPV2 leads specifically to caspase-4-dependent pyroptosis.

Increase in Ca^{2+} influx by extracellular ATP enhances EPEC-1-induced cell death in a caspase-4-dependent manner, while ATP alone does not induce cell death (Zhong et al., 2020). We, therefore, investigated whether Ca^{2+} influx via a different pathway could replace the loss of TRPV2. Control experiments have shown that pre-treating SNU-C5 cells with either ATP or ATP/SET2 similarly induce Ca^{2+} influx (Figure 3d), suggesting the ATP induces Ca^{2+} influx independently of TRPV2. ATP treatment enhanced PI uptake in EPEC-1-infected cells but not uninfected cells, consistent with our previous findings (Figure 3e). Moreover, while SET2 inhibited EPEC-1-induced cell death, this could be circumvented by the addition of ATP (Figure 3e). Combining silencing of caspase-4 with a ATP/SET2 treatment similarly reduced pyroptosis as SET2-treated EPEC-1-infected cells alone (Figure 3e). As a control experiment, we found that SET2 treatment did not further reduce cell death in caspase-4-silenced cells (Figure 3f), consistent with the previous conclusion that TRPV2 and caspase-4 participate in the same signaling pathway. This suggests that while Tir is essential (Figure 3b,c), the role of TRPV2 could be replaced by other Ca^{2+} influx mechanisms.

2.4 | ER transport is required for TRPV2 activation

In resting conditions, TRPV2 resides on the ER membrane. In response to mechanical or chemical stimuli, TRPV2 is transported to the plasma membrane where it becomes activated (Nagasawa et al., 2007). Unfortunately, we were unable to stain for TRPV2 using the commercially available TRPV2 antibody and the transfection efficiency of plasmid pCMV encoding GFP-tagged TRPV2 was too low for robust quantitative analysis (data not shown). However, in order to determine the need for an ER-to-membrane trafficking in EPEC-1-induced TRPV2 activation, we pre-treated SNU-C5 cells with brefeldin A, which inhibits vesicle trafficking between ER and Golgi. A control experiment revealed that brefeldin A treatment slightly reduced cell death following LPS transfection (Figure 4a). In contrast, infection with EPEC-1 resulted in a significant reduction in Ca^{2+} influx and pyroptosis compared to untreated EPEC-1-infected cells (Figure 4b,c), confirming the requirement of ER-to-Golgi transport.

EPEC E2348/69 injects 21 effectors into the host cell, forming a complex signaling network (Garmendia et al., 2005; Ruano-Gallego et al., 2021). It has been shown that the activity of some effectors could be antagonized by others. For example, we have shown that Tir-induced cell death could be mitigated by NleF (Zhong et al., 2020), which inhibits caspase-4 (Blasche et al., 2013; Pallett et al., 2014, 2017). NleA, whose expression and subsequent injection is coupled to Tir translocation (Katsowich et al., 2017), has been shown to bind to the COPII cargo selection protein Sec24 in HeLa cells, where it prevents ER-to-Golgi transport (Thanabalasuriar et al., 2012). We, therefore, hypothesized that NleA might interfere with TRPV2 transport from the ER and prevent EPEC-1-induced

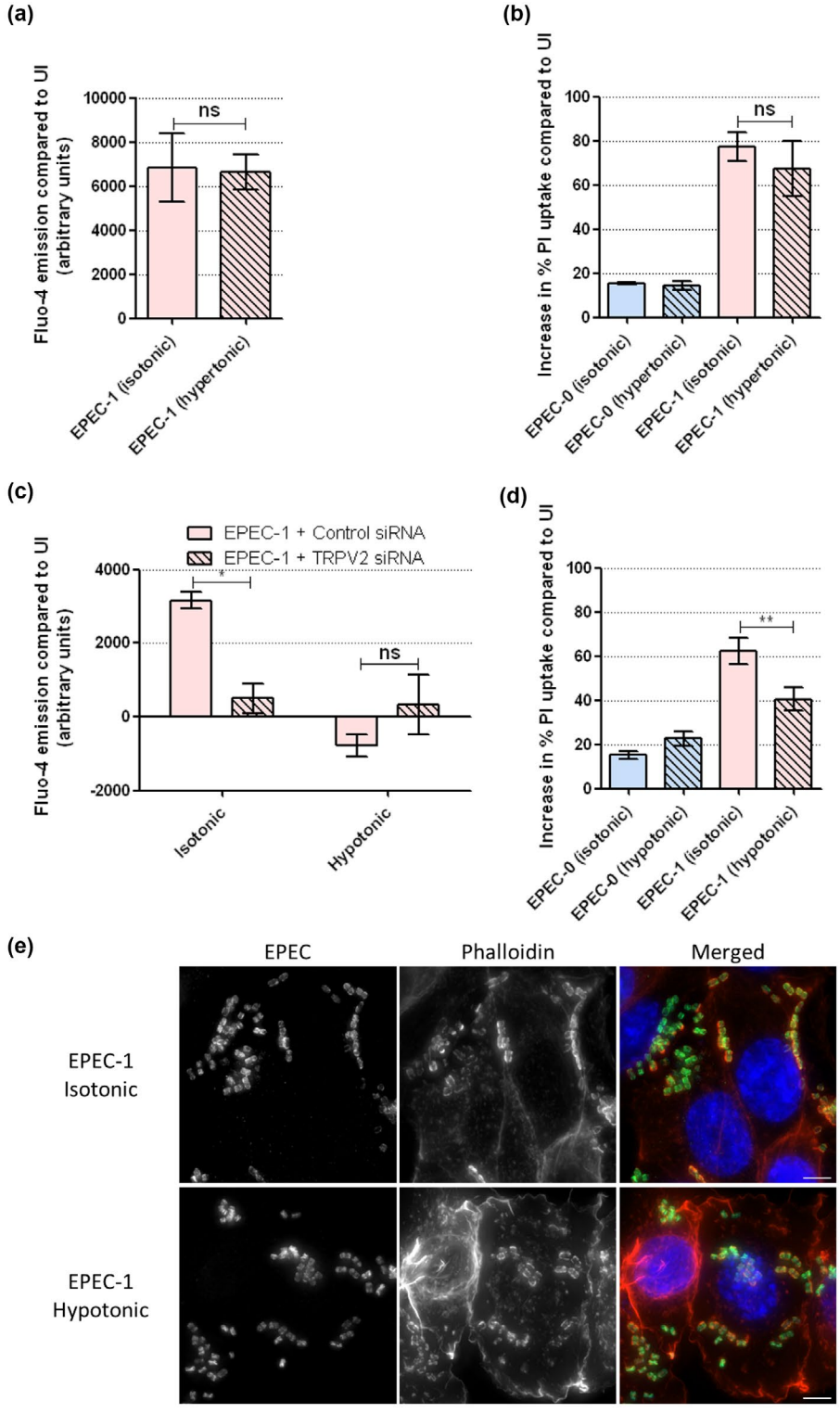

FIGURE 2 Osmolality affects Tir-induced Ca^{2+} influx and pyroptosis. (a) Fluo-4 assay at 20 min after EPEC-1 infection of SNU-C5 cells incubated in isotonic or hypertonic medium. Means ± *SEM* from $n = 3$ independent biological repeats are shown. (b) PI uptake into EPEC-1-infected SNU-C5 cells incubated in isotonic or hypertonic medium. Means ± *SEM* from $n = 3$ independent biological repeats are shown. (c) Fluo-4 assay at 20 min after EPEC-1 infection in control or TRPV2-silenced SNU-C5 cells incubated in isotonic or hypotonic medium. Means ± *SEM* from $n = 3$ independent biological repeats are shown. (d) PI uptake into EPEC-1-infected SNU-C5 cells incubated in isotonic or hypotonic medium. Means ± *SEM* from $n = 6$ independent biological repeats are shown. (e) Immunofluorescence microscopy of EPEC-1-infected SNU-C5 cells incubated in isotonic or hypotonic medium. DAPI: blue; EPEC: green; Phalloidin: red. Scale bar: 5 μm. Shown is a representative image from $n = 3$ independent biological repeats are shown. Statistical significance was determined using two-way ANOVA with Bonferroni post-test. $^{*}p \leq .05$; $^{**}p \leq .01$; $^{***}p \leq .001$; ns, non-significant

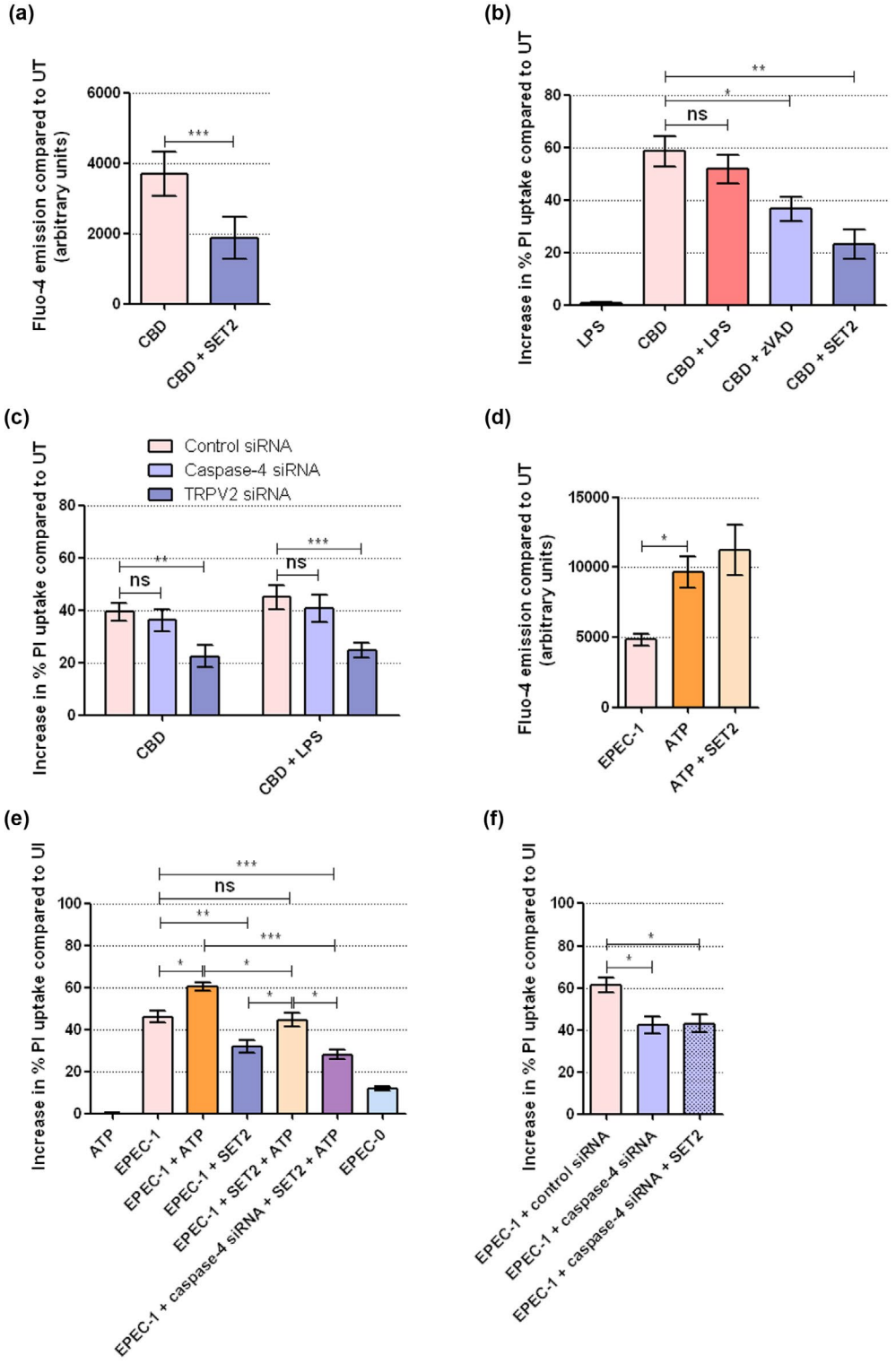

FIGURE 3 Replacing Tir-induced TRPV2 Ca^{2+} influx with pharmacological TRPV2 activation or purinergic Ca^{2+} influx. (a) Fluo-4 assay at 4 min after CBD treatment of SNU-C5 cells, with or without SET2 pre-treatment. UT, untreated. Means ± *SEM* from $n = 5$ independent biological repeats are shown. (b) PI uptake at 2 hr after LPS, CBD, CBD + LPS, CBD + zVAD and CBD + SET2 treatment of SNU-C5 cells. Means ± *SEM* from $n = 3$ independent biological repeats are shown. (c) PI uptake at 2 hr after CBD and CBD + LPS treatment of SNU-C5 cells. Shown are control, caspase-4- or TRPV2-silenced cells. Means ± *SEM* from $n = 4$ independent biological repeats are shown. (d) Fluo-4 assay at 2 min after ATP treatment of SNU-C5 cells, with or without SET2 pre-treatment, and Fluo-4 assay at 20 min post-infection of SNU-C5 cells with EPEC-1. Means ± *SEM* from $n = 3$ independent biological repeats are shown. (e) PI uptake into EPEC-1-infected SNU-C5 cells, with or without SET2 and/or ATP pre-treatment. Shown are control or caspase-4-silenced cells. PI uptake of EPEC-0 infection is included as a negative control. Means ± *SEM* from $n = 3$ independent biological repeats are shown. (f) PI uptake into EPEC-1-infected control or caspase-4 silenced SNU-C5 cells, with or without SET2 pre-treatment. Means ± *SEM* from $n = 3$ independent biological repeats are shown. Statistical significance was determined using 2-tailed *t* test (a), 1-way ANOVA with Tukey post-test (b, d, e, f) or 2-way ANOVA with Bonferroni post-test (c). $^{*}p \leq .05$; $^{**}p \leq .01$; $^{***}p \leq .001$; ns, non-significant

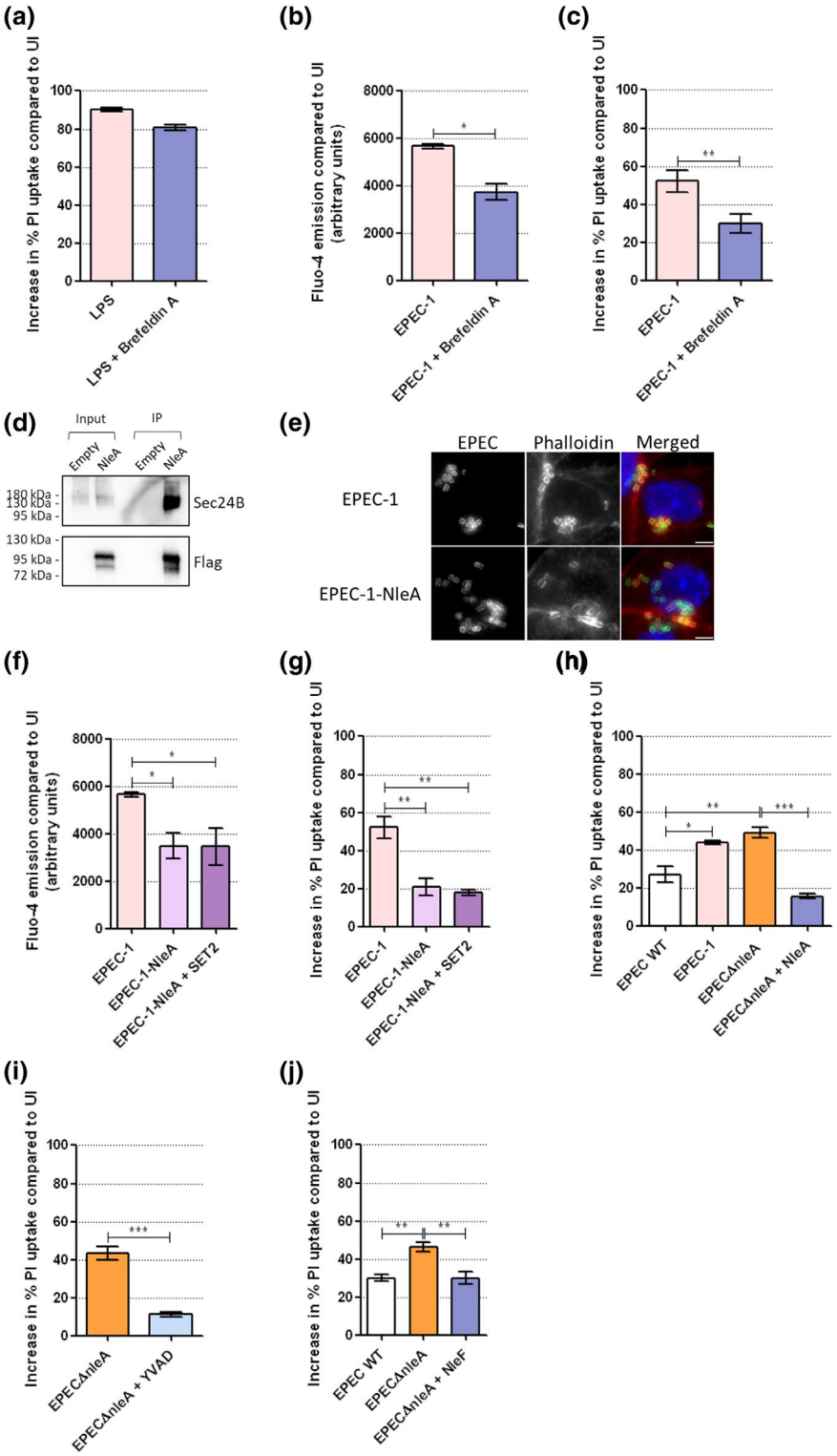

FIGURE 4 Legend on next page

pyroptosis. First, we confirmed that NleA binds Sec24 in SNU-C5 cells. To this end, we infected SNU-C5 cells with EPEC-1 containing a plasmid encoding flag-tagged-NleA (EPEC-1-NleA). Following infection and flag pull-down, we found that Sec24 was co-purified with NleA (Figure 4d). We then confirmed that NleA overexpression did not affect EPEC-1-induced pedestal formation (Figure 4e). Measuring Fluo-4 emission and PI uptake revealed that expression of NleA in EPEC-1 inhibited Ca^{2+} influx and cell death similarly to brefeldin A (Figure 4f,g). A combination of NleA and SET2 did not further reduce EPEC-1-induced Ca^{2+} influx and cell death compared to EPEC-1-NleA alone (Figure 4f,g), implying that the two mechanisms converge.

To further investigate the role of NleA in EPEC-induced pyroptosis, we deleted *nleA* from wild-type (WT) EPEC (EPEC*Δnle*A).

FIGURE 4 ER transport inhibition by brefeldin A and NleA affects TRPV2 activation. (a) PI uptake into LPS-transfected SNU-C5 cells, with or without brefeldin A pre-treatment. Means ± *SEM* from $n = 3$ independent biological repeats are shown. (b) Fluo-4 assay at 20 min after EPEC-1 infection of SNU-C5 cells, with or without brefeldin A pre-treatment. Means ± *SEM* from $n = 3$ independent biological repeats are shown. (c) PI uptake into EPEC-1-infected SNU-C5 cells, with or without brefeldin A pre-treatment. Means ± *SEM* from $n = 3$ independent biological repeats are shown. (d) Western blot of Flag immunoprecipitated lysates (IP) of EPEC-1 pSA10-(EPEC-1 empty) and EPEC-1 pSA10-NleA-Flag-infected SNU-C5 cells, probed with Sec24B and Flag antibodies. Shown is a representative blot from three independent biological repeats. (e) Immunofluorescence microscopy of EPEC-1- and EPEC-1-NleA-infected SNU-C5 cells. DAPI: blue; EPEC: green; Phalloidin: red. Scale bar: 5 μm. (f) PI uptake into EPEC-1- or EPEC-1-NleA-infected SNU-C5 cells, with or without SET2 pre-treatment. Means ± *SEM* from $n = 3$ independent biological repeats are shown. (g) Fluo-4 assay at 20 min after EPEC-1 or EPEC-1-NleA infection of SNU-C5 cells, with or without SET2 pre-treatment. Means ± *SEM* from $n = 3$ independent biological repeats are shown. (h) PI uptake into EPEC WT, EPEC-1, EPEC Δ*nleA* or EPEC Δ*nleA* + NleA-infected SNU-C5 cells. Means ± *SEM* from $n = 3$ independent biological repeats are shown. (i) PI uptake into EPEC Δ*nleA*-infected SNU-C5 cells, with or without YVAD pre-treatment. Means ± *SEM* from $n = 3$ independent biological repeats are shown. (j) PI uptake into EPEC WT, EPEC Δ*nleA* or EPEC Δ*nleA* + NleF-infected SNU-C5 cells. Means ± *SEM* from $n = 4$ independent biological repeats are shown. Statistical significance was determined using two-tailed *t* test (b, c, i) and one-way ANOVA with Tukey post-test (f–h, j). $^{*}p \leq .05$; $^{**}p \leq .01$; $^{***}p \leq .001$; ns, non-significant

Infection of SNU-C5 cells with EPEC Δ*nleA* resulted in an increase in PI uptake to a similar level as EPEC-1; induction of PI uptake could be reversed by complementing EPEC Δ*nleA* with a plasmid encoding NleA (Figure 4h). Using the inhibitor YVAD, we revealed that the mechanism of cell death induced by the EPEC Δ*nleA* was pyroptosis (Figure 4i). Furthermore, overexpression of NleF inhibited EPEC Δ*nleA*-induced cell death, suggesting that NleA and NleF control the same pyroptosis pathway (Figure 4j).

Taken together our data suggest that infection of SNU-C5 cells with EPEC leads to activation of Tir-mediated mechanical stress, trafficking of TRPV2 from the ER to the plasma membrane and Ca^{2+} influx, which promotes LPS entry, followed by caspase-4 activation and pyroptosis. Moreover, EPEC translocates the effectors NleA, and NleF, which inhibit trafficking of TRPV2 and caspase-4 and cell death.

3 | DISCUSSION

We have previously shown that the EPEC T3SS effector Tir triggers extracellular Ca^{2+} influx followed by LPS internalization and caspase-4 activation, culminating in GSDMD-dependent pyroptotic cell death. In this study, we have characterized the mechanisms by which Tir induces Ca^{2+} influx. It was known that the insertion of Tir, followed by Tir-intimin interaction, distorts the local membrane structure, likely via Tir-recruited membrane curvature-inducing proteins such as IRTKS, Eps15, and epsins (Ford et al., 2002; Lin et al., 2011; Vingadassalom et al., 2009; Zhao et al., 2011). Such an event could activate mechanosensitive ion channels. From the proteomics of EPEC-1-infected epithelial cells, we found the mechanosensitive Ca^{2+} channel TRPV2 is highly expressed at resting conditions and shows an increased abundance during infection of SNU-C5 cells (Zhong et al., 2020). Here we have shown that TRPV2 has a critical role in triggering the early Ca^{2+} influx, leading to caspase-4 activation in EPEC-1-infected SNU-C5 cells. Consistent with previous studies on TRPV2, ER transport process is required for TRPV2-dependent Ca^{2+} influx and cell death during EPEC-1 infection. As a mechanosensitive channel, TRPV2 activation can be controlled by changing medium osmolality and the resulting membrane pressure (Muraki et al., 2003; Zanou et al., 2015). In our study, low osmolality inhibited Tir- and TRPV2-induced Ca^{2+} influx and partially reduced cell death. It is likely that Tir activates TRPV2 through membrane structural changes that can be antagonized by the membrane alterations from hypotonic stress. On the other hand, the inability of hypertonic medium to enhance cell death could be explained by the necessity of a localized structural distortion to activate TRPV2 rather than a global cell shape change.

Cytosolic Ca^{2+} overload has been associated extensively with different cell death mechanisms. Ca^{2+} influx into the cytosol can be from either an extracellular or an intracellular source. Extracellular Ca^{2+} influx mediated by plasma membrane ion channels, such as TRP family, purinergic and voltage-gated Ca^{2+} channels, can lead to Ca^{2+} uptake by organelles including ER, mitochondria, and lysosomes (Kondratskyi et al., 2015). ER can also relay Ca^{2+} directly into adjacent mitochondria or release Ca^{2+} to promote mitochondrial uptake, triggering the cell death signaling (Joseph & Hajnóczky, 2007; Marchi et al., 2018; Min et al., 2012). Ca^{2+} overloading of mitochondria causes mitochondrial outer membrane permeability, cytochrome C release, and mitochondrial ROS production, which participate in intrinsic apoptosis (Gogvadze et al., 2006; Tait & Green, 2013). Furthermore, Ca^{2+} influx, mitochondrial ROS production, and mitochondrial DNA release have been implicated in the canonical NLRP3 inflammasome formation (Broz & Dixit, 2016; Murakami et al., 2012; Shimada et al., 2012; Zhou et al., 2011). Early studies of caspase-4 activation have also suggested the role of Ca^{2+} influx from stressed ER (Matsuzaki et al., 2010). Our discovery of TRPV2 upstream of caspase-4 activation makes the first connection between the non-canonical inflammasome and a specific plasma membrane Ca^{2+} channel.

It remains unclear how TRPV2-dependent Ca^{2+} influx leads to LPS entry. Although pharmacological activation of TRPV2 leads to cell lysis, LPS and caspase-4 appear to be dispensable in this pathway. Therefore, Tir appears to play a key role by promoting LPS entry and changing the caspase preference downstream of TRPV2. Both the intimin-Tir cluster and TRPV2 have been shown to be recruited to lipid rafts for their respective functions (Allen-Vercoe et al., 2006; Lévêque et al., 2018). Similarly, scavenger receptors capable of transporting LPS, such as SR-BI expressed in SNU-C5 (Roumeliotis et al., 2017), are also found

in lipid rafts (Peng et al., 2004; Plebanek et al., 2015; Vishnyakova et al., 2003). Intimin-Tir cluster and TRPV2-dependent Ca^{2+} influx may function in close proximity in the LPS internalization process.

Tir-induced TRPV2 activation, which requires ER transport, is blocked by the effector NleA that binds to Sec24 and prevents ER-to-Golgi transport (Kim et al., 2007; Thanabalasuriar et al., 2012). It is interesting to note that while having an antagonistic function the injection of NleA is coupled to Tir translocations (Katsowich et al., 2017). In addition to NleA, we have previously shown that EspZ reduces Tir translocation while NleF inhibits caspase-4 (Berger et al., 2012; Pallett et al., 2014, 2017), all leading to reduced pyroptosis in SNU-C5 (Zhong et al., 2020). Increased pyroptosis due to loss of NleA in WT EPEC can be complemented by NleF, showing their redundant roles in pyroptosis inhibition. Importantly, in the *Citrobacter rodentium* mouse model of EPEC infection, NleA is one of the three essential effectors that could not be deleted without causing significant attenuation (Ruano-Gallego et al., 2021); it remains to be seen if the main activity of NleA in vivo is to block the side effect induced by Tir membrane integration. The relationship between NleA and NleF is reminiscent to that of NleE and NleC which block the top and bottom of the NF-kB cascade, respectively (Nadler et al., 2010; Sham et al., 2011).

Pyroptosis in infected cells can release pro-inflammatory cytokines such as IL-1β and IL-18 as well as DAMPs to activate immune cells and trap pathogenic bacteria, promoting bacterial clearance (Eldridge & Shenoy, 2015; Jorgensen et al., 2016). In *C. rodentium*-infected mice, deletion of inflammasome components in non-hemopoietic intestinal cells leads to increased bacterial colonization, penetration into the crypt base and dissemination to the spleen, accompanied by exacerbated intestinal inflammation (Song-Zhao et al., 2014). Our results emphasize that pyroptosis in the host cell is likely not favored by the EPEC pathogen (or alternatively, favored by the host) as multiple mechanisms are leveraged by the bacteria to block the pyroptosis signaling downstream of a single effector. Overall, we have characterized the involvement of the mechanosensitive Ca^{2+} influx via TRPV2 in Tir-induced pyroptosis and its regulation by other effectors intracellularly.

4 | EXPERIMENTAL PROCEDURES

4.1 | Bacterial strains and cell lines

EPEC E2348/69 strains (Table S1) were grown in Luria Bertani (LB) (Sigma-Aldrich, St. Louis, Missouri, United States of America) broth or agar. Overnight bacterial cultures were grown at 37°C, 180 rpm shaking (liquid) or static (agar), and primed in Dulbecco's modified eagle medium (DMEM) as described below for infections.

SNU-C5 cells were cultured in Roswell Park Memorial Institute (RPMI) medium (Sigma) with 10% (v/v) fetal bovine serum (FBS) (Gibco, Carlsbad, California, USA), 2 mM Glutamax (Gibco), 1 mM sodium pyruvate (Sigma), 10 mM N-2-hydroxyethylpiperazine-N-2-ethane sulphonic acid (HEPES) (Sigma) and 2500 μg/ml glucose (Sigma).

4.2 | EPEC-1 and EPECΔ*nleA* expressing plasmid-encoded NleA or NleF

EPEC NleA with 3-×FLAG-TwinStrepII tag at C-terminus was synthesized by GeneArt (Thermo Fisher, Waltham, Massachusetts, USA). The fragment was inserted into pSA10 plasmid to generate pSA10-*nleA*-Flag. pSA10 (empty plasmid), pSA10-*nleA*-Flag or pACYC-*nleF* (Pallett et al., 2017) (Table S2) was electroporated into EPEC-1 or EPECΔ*nleA*.

4.3 | Infection of SNU-C5 cells

EPEC infection of SNU-C5 cells was performed as described before in (Zhong et al., 2020) with modifications. Briefly, EPEC strains were primed by diluting the overnight cultures 50× in non-supplemented DMEM (low glucose) and growing for 3 hr static at 37°C with 5% CO_2. Isopropyl β-D-1-thiogalactopyranoside (IPTG) (Sigma) at 0.5 mM was added to the bacterial culture 30 min before infection when required. Infection was carried out at a multiplicity-of-infection (MOI) of 50:1. Spent medium was replaced with fresh serum-free RPMI 1 hr before infection to avoid serum-induced TRPV2 activation (Nagasawa et al., 2007). Alternatively, isotonic (~290 mOs/kg) and hypotonic (~100 mOs/kg) medium was prepared using RPMI adjusted by 1 M sorbitol (Sigma) and water supplemented with $CaCl_2$ (Sigma) to a final concentration of 0.42 mM. Cells were incubated in isotonic and hypotonic medium for 30 min before infection. Infected cells were centrifuged at 700 *g* for 10 min and incubated for 2 hr static at 37°C, 5% CO_2. For over 2 hr of infection, 200 μg/ml gentamicin (Sigma) was added 2 hr post-infection.

4.4 | Cytokine and drug treatment

10 ng/ml human recombinant-IFNγ (R&D Systems, Minneapolis, Minnesota, USA) was added to the cells 24 hr before infection.

50 μM zVAD-fmk (zVAD) (R&D), 50 μM zYVAD-fmk (YVAD) (R&D), 1 mM EGTA (Sigma), 10 μM SET2 (Tocris, Bristol, UK), 0.5 mM ATP (Sigma) and 1 μg/ml brefeldin A (Sigma) was added to the cells 30 min before infection. Thirty-micromolar cannabidiol (CBD) was used with or without 5 μg/ml Ultrapure *E. coli* O111:B4 LPS (Invivogen, San Diego, California, USA) extracellularly. Ultrapure *E. coli* O111:B4 LPS transfection was performed using Lipofectamine 2000 at 5 μg/ml.

4.5 | siRNA transfection

1.25×10^4 cells/well were seeded in black clear-bottom 96-well plates 3 days prior to infection. 50 mM siRNA (0.25 μl) (Table S3) (Dharmacon, Lafayette, Colorado, USA) mixed with 0.3 μl of TransIT-X2 transfection reagent (Mirus Bio, Madison, Wisconsin, USA) in 9 μl Opti-MEM were added to the cells 6 hr after seeding.

Medium was replaced with fresh RPMI with a second siRNA dose of identical concentration 24 hr after the first dose. Medium was replaced with IFNγ-containing RPMI one day before infection.

4.6 | qRT-PCR

5×10^4 cells/well were seeded in 24-well plates three days prior to RNA extraction. RNA extraction and qRT-PCR were performed as described before (Zhong et al., 2020). Briefly, RNAeasy kit (QIAGEN) and RQ1 RNase-free DNase (Qiagen) were used for RNA extraction and DNase digestion. M-MLV reverse transcriptase (Promega) and oligo-dT and random primers (Promega, Madison, Wisconsin, USA) were used to perform the RT reaction at 42°C for 60 min. PowerUp SyBr-Green Mastermix and gene-specific primers (Figure S4) were used to perform qPCR reaction in a StepOne Real-Time PCR system (Thermo). TRPV2 cDNA-specific primer sequences were from Caprodossi et al. (2008). GAPDH cDNA level was used as an internal control.

4.7 | Immunofluorescence staining

1.5×10^5 cells/well were seeded in 24-well plates on glass coverslips for imaging with Zeiss AxioImager Z1 microscope (Carl Zeiss, Jena, Germany). Infection experiments were carried out as described. Infected cells were fixed and stained as described before in Zhong et al. (2020). Briefly, cells were fixed by 4% paraformaldehyde, permeabilized by 0.2% Triton X-100 (Sigma), blocked for 10 min with 1% bovine serum albumin (BSA) before being incubated with primary antibodies for 45 min, and re-blocked for 10 min with 1% BSA before being incubated with secondary antibodies for 30 min (Table S5). Coverslips were mounted on glass slides with Gold-Pro-Long-Antifade (Invitrogen) before imaging.

4.8 | In vitro infection and pulldown

For pulldown experiments, 3×10^5 cells/well were seeded in six-well plates. After priming the EPEC-1 empty vector and EPEC-1-NleA strains, 0.5 mM IPTG was used to induce NleA expression 30 min prior to infection. After 2 hr, cells were washed thrice in PBS followed by cell lysis (50 mM Tris–HCl, pH 7.4, with 150 mM NaCl, 1 mM EDTA, and 1% Triton X-100, protease inhibitor cocktail). The lysate was subjected to binding to Anti-FLAG M2 affinity resin as per the manufacturer's instructions. Briefly, bead binding was performed for 4 hr at 4°C. For western blotting, the beads were boiled with non-reduced Laemmli buffer to elute the bound proteins and subjected to western blot analysis.

4.9 | Western blotting

Western blotting was performed as described before in Zhong et al. (2020). Cells were lysed with lysis buffer containing radioimmunoprecipitation (RIPA) buffer (50 mM Tris-HCl, pH 8, 2 mM EDTA, 300 mM NaCl, 2% NP-40, 1% sodium deoxycholate) and 1× Protease Inhibitor (Pierce, Waltham, Massachusetts, USA) and mixed with 1× Laemmli loading dye (Bio-Rad, Hercules, California, USA) and 5% β-mercaptoethanol (Sigma). Alternatively for pulldown, samples were prepared as described above. Lysates and pulldown samples were run on sodium dodecyl sulfate polyacrylamide gel electrophoresis (SDS-PAGE) gels and TransBlot Turbo Transfer System (Bio-Rad) was used to transfer the protein bands to the polyvinylidene difluoride (PVDF) membrane (Bio-Rad). Membranes were blocked with 3% BSA or 5% milk in TBST or PBST for 1 hr at room temperature and incubated with primary antibodies overnight at 4°C, followed by secondary antibodies for 1 hr at room temperature (Table S6). Membranes were developed using the ECL Western Blotting Reagents (GE, Amersham, UK) and imaged using the ChemiDoc MP imaging system (Bio-Rad).

4.10 | PI-uptake assay

5×10^4 cells/well were seeded in black clear-bottom 96-well plates one day prior to infection and IFNγ and inhibitor treatment were applied as described above. Alternatively, 1.5×10^4 cells/well were seeded three days prior to infection for siRNA transfection. PI-uptake assay was performed as described before in Zhong et al. (2020). Briefly, phenol-red-free DMEM (low glucose) and RPMI was used for T3SS priming and infection, respectively. Cells were incubated in phenol-red-free RPMI supplemented with 5 μg/ml PI (Sigma) 1 hr prior to infection and throughout the infection. Alternatively, phenol-red-free RPMI with osmolality adjusted by sorbitol and water as described above and supplemented with 5 μg/ml PI was used. Cell-free medium-only wells were prepared as blank. Positive control wells were prepared by incubating cells in RPMI with 5 μg/ml PI and 0.05% Triton X-100 (Sigma) 10 min prior to infection. Infections were carried out as described above. Measurement was taken with 620-nm emission and 520-nm excitation using the FLUOstar Omega Microplate Reader (BMG Labtech, Aylesbury, UK).

4.11 | Fluo-4 assay

5×10^4 cells/well were seeded in black clear-bottom 96-well plates one day prior to infection and IFNγ was applied as described above. Fluo-4 assay was performed as described before in Zhong et al. (2020). Briefly, cells were incubated in Fluo-4 Direct reagent (Molecular Probes, Eugene, Oregon, USA) diluted two-fold in phenol-red-free RPMI for 30 min before the first measurement. Alternatively, 25% Fluo-4 Direct reagent was used to prepare isotonic and hypotonic medium adjusted by sorbitol and water. Cell-free medium-only wells were prepared as blank. Fluorescence readings were performed in the FLUOstar Omega Microplate Reader (BMG Labtech, Aylesbury, UK) measuring 520-nm emission with 485-nm excitation.

4.12 | Statistical analysis

All experiments were independently repeated at least three times as indicated in the figure legends. Methods of data transformation are described in their corresponding method sections.

Statistical analysis of all biochemical/biological experimental data was performed using GraphPad Prism 5.1. Student's *t*-test, one-way or two-way analysis of variance (ANOVA) followed by Tukey post-test or Bonferroni post-test, respectively, were performed on the means as listed in the figure legends. Significant result was defined as having a p-value $<.05$.

ACKNOWLEDGMENTS

We thank Luis Ángel Fernández of CNB-CSIC, Madrid, for sharing EPEC-0 and EPEC-1. QZ is supported by an Imperial College President's PhD Scholarship. The project was supported by a grant from the Wellcome Trust (107057/Z/15/Z).

CONFLICT OF INTEREST

The authors declare no conflict.

DATA AVAILABILITY STATEMENT

Data sharing not applicable to this article as no datasets were generated or analysed during the current study.

ORCID

Qiyun Zhong https://orcid.org/0000-0001-7053-9640
Sharanya Chatterjee https://orcid.org/0000-0002-5806-6278
Jyoti S. Choudhary https://orcid.org/0000-0003-0881-5477
Gad Frankel https://orcid.org/0000-0002-0046-1363

REFERENCES

Allen-Vercoe, E., Waddell, B., Livingstone, S., Deans, J. & DeVinney, R. (2006) Enteropathogenic *Escherichia coli* Tir translocation and pedestal formation requires membrane cholesterol in the absence of bundle-forming pili. *Cellular Microbiology*, *8*, 613–624. https://doi.org/10.1111/j.1462-5822.2005.00654.x

Berger, C.N., Crepin, V.F., Baruch, K., Mousnier, A., Rosenshine, I. & Frankel, G. (2012) EspZ of enteropathogenic and enterohemorrhagic *Escherichia coli* regulates type III secretion system protein translocation. *MBio*, *3*, 1–12. https://doi.org/10.1128/mBio.00317-12

Blasche, S., Mortl, M., Steuber, H., Siszler, G., Nisa, S., Schwarz, F. et al. (2013) The *E. coli* effector protein NleF is a caspase inhibitor. *PLoS One*, *8*, e58937. https://doi.org/10.1371/journal.pone.0058937

Bommarius, B., Maxwell, D., Swimm, A., Leung, S., Corbett, A., Bornmann, W. et al. (2007) Enteropathogenic *Escherichia coli* Tir is an SH2/3 ligand that recruits and activates tyrosine kinases required for pedestal formation. *Molecular Microbiology*, *63*, 1748–1768. https://doi.org/10.1111/j.1365-2958.2007.05626.x

Brady, M.J., Campellone, K.G., Ghildiyal, M. & Leong, J.M. (2007) Enterohaemorrhagic and enteropathogenic *Escherichia coli* Tir proteins trigger a common Nck-independent actin assembly pathway. *Cellular Microbiology*, *9*, 2242–2253. https://doi.org/10.1111/j.1462-5822.2007.00954.x

Broz, P. & Dixit, V.M. (2016) Inflammasomes: mechanism of assembly, regulation and signalling. *Nature Reviews Immunology*, *16*, 407–420. https://doi.org/10.1038/nri.2016.58

Campellone, K.G. & Leong, J.M. (2005) Nck-independent actin assembly is mediated by two phosphorylated tyrosines within enteropathogenic *Escherichia coli* Tir. *Molecular Microbiology*, *56*, 416–432. https://doi.org/10.1111/j.1365-2958.2005.04558.x

Campellone, K.G., Rankin, S., Pawson, T., Kirschner, M.W., Tipper, D.J. & Leong, J.M. (2004) Clustering of Nck by a 12-residue Tir phosphopeptide is sufficient to trigger localized actin assembly. *Journal of Cell Biology*, *164*, 407–416. https://doi.org/10.1083/jcb.200306032

Caprodossi, S., Lucciarini, R., Amantini, C., Nabissi, M., Canesin, G., Ballarini, P. et al. (2008) Transient receptor potential vanilloid type 2 (TRPV2) expression in normal urothelium and in urothelial carcinoma of human bladder: correlation with the pathologic stage. *European Urology*, *54*, 612–620. https://doi.org/10.1016/j.eururo.2007.10.016

Caterina, M.J., Rosen, T.A., Tominaga, M., Brake, A.J. & Julius, D. (1999) A capsaicin-receptor homologue with a high threshold for noxious heat. *Nature*, *398*, 436–441. https://doi.org/10.1038/18906

Chai, H., Cheng, X.I., Zhou, B., Zhao, L., Lin, X., Huang, D. et al. (2019) Structure-based discovery of a subtype-selective inhibitor targeting a transient receptor potential vanilloid channel. *Journal of Medicinal Chemistry*, *62*, 1373–1384. https://doi.org/10.1021/acs.jmedchem.8b01496

Chen, H.D. & Frankel, G. (2005) Enteropathogenic *Escherichia coli*: unravelling pathogenesis. *FEMS Microbiology Reviews*, *29*, 83–98. https://doi.org/10.1016/j.femsre.2004.07.002

Eldridge, M.J.G. & Shenoy, A.R. (2015) Antimicrobial inflammasomes: unified signalling against diverse bacterial pathogens. *Current Opinion in Microbiology*, *23*, 32–41. https://doi.org/10.1016/j.mib.2014.10.008

Fisch, D., Bando, H., Clough, B., Hornung, V., Yamamoto, M., Shenoy, A.R. et al. (2019) Human GBP1 is a microbe-specific gatekeeper of macrophage apoptosis and pyroptosis. *EMBO Journal*, *38*, e100926. https://doi.org/10.15252/embj.2018100926

Ford, M.G.J., Mills, I.G., Peter, B.J., Vallis, Y., Praefcke, G.J.K., Evans, P.R. et al. (2002) Curvature of clathrin-coated pits driven by epsin. *Nature*, *419*, 361–366. https://doi.org/10.1038/nature01020

Frankel, G., Phillips, A.D., Trabulsi, L.R., Knutton, S., Dougan, G. & Matthews, S. (2001) Intimin and the host cell – is it bound to end in Tir(s)? *Trends in Microbiology*, *9*, 214–218. https://doi.org/10.1016/S0966-842X(01)02016-9

Garmendia, J., Frankel, G. & Crepin, V.F. (2005) Enteropathogenic and enterohemorrhagic *Escherichia coli* infections: translocation, translocation, translocation. *Infection and Immunity*, *73*, 2573–2585. https://doi.org/10.1128/IAI.73.5.2573-2585.2005

Goddard, P.J., Sanchez-Garrido, J., Slater, S.L., Kalyan, M., Ruano-Gallego, D., Marchès, O. et al. (2019) Enteropathogenic *Escherichia coli* stimulates effector-driven rapid caspase-4 activation in human macrophages. *Cell Reports*, *27*, 1008–1017. https://doi.org/10.1016/j.celrep.2019.03.100

Gogvadze, V., Orrenius, S. & Zhivotovsky, B. (2006) Multiple pathways of cytochrome c release from mitochondria in apoptosis. *Biochimica et Biophysica Acta - Bioenergetics*, *1757*, 639–647. https://doi.org/10.1016/j.bbabio.2006.03.016

Gruenheid, S., DeVinney, R., Bladt, F., Goosney, D., Gelkop, S., Gish, G.D. et al. (2001) Enteropathogenic *E. coli* Tir binds Nck to initiate actin pedestal formation in host cells. *Nature Cell Biology*, *3*, 856–859. https://doi.org/10.1038/ncb0901-856

Hayward, R.D., Hume, P.J., Humphreys, D., Phillips, N., Smith, K. & Koronakis, V. (2009) Clustering transfers the translocated *Escherichia coli* receptor into lipid rafts to stimulate reversible activation of c-Fyn. *Cellular Microbiology*, *11*, 433–441. https://doi.org/10.1111/j.1462-5822.2008.01265.x

Jorgensen, I., Rayamajhi, M. & Miao, E.A. (2016) Programmed cell death as a defence against infection. *Nature Reviews Immunology*, *42*, 407–420. https://doi.org/10.1038/nri.2016.147

Joseph, S.K. & Hajnóczky, G. (2007) IP3 receptors in cell survival and apoptosis: Ca^{2+} release and beyond. *Apoptosis*, *12*, 951–968. https://doi.org/10.1007/s10495-007-0719-7

Kalman, D., Weiner, O., Goosney, D., Sedat, J., Finlay, B., Abo, A. et al. (1999) Enteropathogenic *E. coli* acts through WASP and Arp2/3 complex to form actin pedestals. *Nature Cell Biology*, *1*, 389–391. https://doi.org/10.1038/14087

Kanzaki, M., Zhang, Y., Mashima, H., Li, L., Shibata, H. & Kojima, I. (1999) Translocation of a calcium-permeable cation channel induced by insulin-like growth factor-I. *Nature Cell Biology*, *1*, 165–170. https://doi.org/10.1038/11086

Katsowich, N., Elbaz, N., Pal, R.R., Mills, E., Kobi, S., Kahan, T. et al. (2017) Host cell attachment elicits posttranscriptional regulation in infecting enteropathogenic bacteria. *Science*, *355*, 735–739. https://doi.org/10.1126/science.aah4886

Kayagaki, N., Stowe, I.B., Lee, B.L., O'Rourke, K., Anderson, K., Warming, S. et al. (2015) Caspase-11 cleaves gasdermin D for non-canonical inflammasome signalling. *Nature*, *526*, 666–671. https://doi.org/10.1038/nature15541

Kayagaki, N., Wong, M.T., Stowe, I.B., Ramani, S.R., Gonzalez, L.C., Akashi-Takamura, S. et al. (2013) Noncanonical inflammasome activation by intracellular LPS independent of TLR4. *Science*, *341*, 1246–1249. https://doi.org/10.1126/science.1240248

Kenny, B., DeVinney, R., Stein, M., Reinscheid, D.J., Frey, E.A. & Finlay, B.B. (1997) Enteropathogenic *E. coli* (EPEC) transfers its receptor for intimate adherence into mammalian cells. *Cell*, *91*, 511–520. https://doi.org/10.1016/S0092-8674(00)80437-7

Kim, J., Thanabalasuriar, A., Chaworth-Musters, T., Fromme, J.C., Frey, E.A., Lario, P. et al. (2007) The bacterial virulence factor NleA inhibits cellular protein secretion by disrupting mammalian COPII function. *Cell Host and Microbe*, *2*, 160–171. https://doi.org/10.1016/j.chom.2007.07.010

Kondratskyi, A., Kondratska, K., Skryma, R. & Prevarskaya, N. (2015) Ion channels in the regulation of apoptosis. *Biochimica et Biophysica Acta - Biomembranes*, *1848*, 2532–2546. https://doi.org/10.1016/j.bbamem.2014.10.030

Lévêque, M., Penna, A., Le Trionnaire, S., Belleguic, C., Desrues, B., Brinchault, G. et al. (2018) Phagocytosis depends on TRPV2-mediated calcium influx and requires TRPV2 in lipids rafts: alteration in macrophages from patients with cystic fibrosis. *Scientific Reports*, *8*, 1–13. https://doi.org/10.1038/s41598-018-22558-5

Lin, A.E., Benmerah, A. & Guttman, J.A. (2011) Eps15 and epsin1 are crucial for enteropathogenic *Escherichia coli* pedestal formation despite the absence of adaptor protein 2. *Journal of Infectious Diseases*, *204*, 695–703. https://doi.org/10.1093/infdis/jir386

Liu, C. & Montell, C. (2015) Forcing open TRP channels: mechanical gating as a unifying activation mechanism. *Biochemical and Biophysical Research Communications*, *460*, 22–25. https://doi.org/10.1016/j.bbrc.2015.02.067

Marchi, S., Patergnani, S., Missiroli, S., Morciano, G., Rimessi, A., Wieckowski, M.R. et al. (2018) Mitochondrial and endoplasmic reticulum calcium homeostasis and cell death. *Cell Calcium*, *69*, 62–72. https://doi.org/10.1016/j.ceca.2017.05.003

Matsuzaki, S., Hiratsuka, T., Kuwahara, R., Katayama, T. & Tohyama, M. (2010) Caspase-4 is partially cleaved by calpain via the impairment of Ca^{2+} homeostasis under the ER stress. *Neurochemistry International*, *56*, 352–356. https://doi.org/10.1016/j.neuint.2009.11.007

Min, C., Yeom, D., Lee, K.-E., Kwon, H.-K., Kang, M., Kim, Y.-S. et al. (2012) Coupling of ryanodine receptor 2 and voltage-dependent anion channel 2 is essential for Ca^{2+} transfer from the sarcoplasmic reticulum to the mitochondria in the heart. *Biochemical Journal*, *447*, 371–379. https://doi.org/10.1042/BJ20120705

Monet, M., Gkika, D., Lehen'kyi, V., Pourtier, A., Abeele, F.V., Bidaux, G. et al. (2009) Lysophospholipids stimulate prostate cancer cell migration via TRPV2 channel activation. *Biochimica et Biophysica Acta*, *1793*, 528–539. https://doi.org/10.1016/j.bbamcr.2009.01.003

Murakami, T., Ockinger, J., Yu, J., Byles, V., McColl, A., Hofer, A.M. et al. (2012) Critical role for calcium mobilization in activation of the NLRP3 inflammasome. *Proceedings of the National Academy of Sciences*, *109*, 11282–11287. https://doi.org/10.1073/pnas.1117765109

Muraki, K., Iwata, Y., Katanosaka, Y., Ito, T., Ohya, S., Shigekawa, M. et al. (2003) TRPV2 is a component of osmotically sensitive cation channels in murine aortic myocytes. *Circulation Research*, *93*, 829–838. https://doi.org/10.1161/01.RES.0000097263.10220.0C

Nadler, C., Baruch, K., Kobi, S., Mills, E., Haviv, G., Farago, M. et al. (2010) The type III secretion effector NleE inhibits NF-κB activation. *PLoS Path*, *6*, e1000743. https://doi.org/10.1371/journal.ppat.1000743

Nagasawa, M. & Kojima, I. (2015) Translocation of TRPV2 channel induced by focal administration of mechanical stress. *Physiological Reports*, *3*, 1–12. https://doi.org/10.14814/phy2.12296

Nagasawa, M., Nakagawa, Y., Tanaka, S. & Kojima, I. (2007) Chemotactic peptide fMetLeuPhe induces translocation of the TRPV2 channel in macrophages. *Journal of Cellular Physiology*, *210*, 692–702. https://doi.org/10.1002/jcp.20883

Pallett, M.A., Berger, C.N., Pearson, J.S., Hartland, E.L. & Frankel, G. (2014) The type III secretion effector NleF of enteropathogenic *Escherichia coli* activates NF-κB early during infection. *Infection and Immunity*, *82*, 4878–4888. https://doi.org/10.1128/IAI.02131-14

Pallett, M.A., Crepin, V.F., Serafini, N., Habibzay, M., Kotik, O., Sanchez-Garrido, J. et al. (2017) Bacterial virulence factor inhibits caspase-4/11 activation in intestinal epithelial cells. *Mucosal Immunology*, *10*, 602–612. https://doi.org/10.1038/mi.2016.77

Peng, Y., Akmentin, W., Connelly, M., Lund-Katz, S., Phillips, M. & Williams, D. (2004) Scavenger receptor BI (SR-BI) clustered on microvillar extensions suggests that this plasma membrane domain is a way station for cholesterol trafficking between cells and high-density lipoprotein. *Molecular Biology of the Cell*, *15*, 384–396. https://doi.org/10.1091/mbc.e03-06-0445

Petrocellis, L.D., Ligresti, A., Moriello, A.S., Allarà, M., Bisogno, T., Petrosino, S. et al. (2011) Effects of cannabinoids and *Cannabis* extracts on TRP channels and endocannabinoid. *British Journal of Pharmacology*, *163*, 1479–1494. https://doi.org/10.1111/j.1476-5381.2010.01166.x

Phillips, N., Hayward, R.D. & Koronakis, V. (2004) Phosphorylation of the enteropathogenic *E. coli* receptor by the Src-family kinase c-Fyn triggers actin pedestal formation. *Nature Cell Biology*, *6*, 618–625. https://doi.org/10.1038/ncb1148

Plebanek, M.P., Mutharasan, R.K., Volpert, O., Matov, A., Gatlin, J.C. & Thaxton, C.S. (2015) Nanoparticle targeting and cholesterol flux through scavenger receptor type B-1 inhibits cellular exosome uptake. *Scientific Reports*, *5*, 1–14. https://doi.org/10.1038/srep15724

Reichhart, N., Keckeis, S., Fried, F., Fels, G. & Strauss, O. (2015) Regulation of surface expression of TRPV2 channels in the retinal pigment epithelium. *Graefe's Archive for Clinical and Experimental Ophthalmology*, *253*, 865–874. https://doi.org/10.1007/s00417-014-2917-7

Rohatgi, R., Nollau, P., Ho, H.-Y.-H., Kirschner, M.W. & Mayer, B.J. (2001) Nck and phosphatidylinositol 4,5-bisphosphate synergistically activate actin polymerization through the N-WASP-Arp2/3 pathway. *Journal of Biological Chemistry*, *276*, 26448–26452. https://doi.org/10.1074/jbc.M103856200

Roumeliotis, T.I., Williams, S.P., Gonçalves, E., Alsinet, C., Del Castillo Velasco-Herrera, M., Aben, N. et al. (2017) Genomic determinants of protein abundance variation in colorectal cancer cells. *Cell Reports*, *20*, 2201–2214. https://doi.org/10.1016/j.celrep.2017.08.010

Ruano-Gallego, D., Sanchez-Garrido, J., Kozik, Z., Núñez-Berrueco, E., Cepeda-Molero, M., Mullineaux-Sanders, C. et al. (2021) Type III secretion system effectors form robust and flexible intracellular virulence networks. *Science*, *371*. https://doi.org/10.1126/science.abc9531

Sanchez-Garrido, J., Slater, S.L., Clements, A., Shenoy, A.R. & Frankel, G. (2020) Vying for the control of inflammasomes: the cytosolic frontier of enteric bacterial pathogen–host interactions. *Cellular Microbiology*, *22*, e13184. https://doi.org/10.1111/cmi.13184

Santos, J.C., Boucher, D., Schneider, L.K., Demarco, B., Dilucca, M., Shkarina, K. et al. (2020) Human GBP1 binds LPS to initiate assembly of a caspase-4 activating platform on cytosolic bacteria. *Nature Communications*, *11*, 3276. https://doi.org/10.1038/s41467-020-16889-z

Sason, H., Milgrom, M., Weiss, A.M., Melamed-Book, N., Balla, T., Grinstein, S. et al. (2009) Enteropathogenic *Escherichia coli* subverts phosphatidylinositol 4,5-bisphosphate and phosphatidylinositol 3,4,5-trisphosphate upon epithelial cell infection. *Molecular Biology of the Cell*, *20*, 544–555. https://doi.org/10.1091/mbc.e08-05-0516

Sham, H.P., Shames, S.R., Croxen, M.A., Ma, C., Chan, J.M., Khan, M.A. et al. (2011) Attaching and effacing bacterial effector NleC suppresses epithelial inflammatory responses by inhibiting NF-κB and p38 mitogen-activated protein kinase activation. *Infection and Immunity*, *79*, 3552–3562. https://doi.org/10.1128/IAI.05033-11

Shenoy, A.R., Furniss, C.D., Goddard, P.J. & Clements, A. (2018) Modulation of host cell processes by T3SS effectors. *Current Topics in Microbiology and Immunology*, *416*, 73–115. https://doi.org/10.1007/82_2018_106

Shi, J., Zhao, Y., Wang, K., Shi, X., Wang, Y., Huang, H. et al. (2015) Cleavage of GSDMD by inflammatory caspases determines pyroptotic cell death. *Nature*, *526*, 660–665. https://doi.org/10.1038/nature15514

Shimada, K., Crother, T., Karlin, J., Dagvadorj, J., Chiba, N., Chen, S. et al. (2012) Oxidized mitochondrial DNA activates the NLRP3 inflammasome during apoptosis. *Immunity*, *36*, 401–414. https://doi.org/10.1016/j.immuni.2012.01.009

Song-Zhao, G.X., Srinivasan, N., Pott, J., Baban, D., Frankel, G. & Maloy, K.J. (2014) Nlrp3 activation in the intestinal epithelium protects against a mucosal pathogen. *Mucosal Immunology*, *7*, 763–774. https://doi.org/10.1038/mi.2013.94

Startek, J.B., Boonen, B., Talavera, K. & Meseguer, V. (2019) TRP channels as sensors of chemically-induced changes in cell membrane mechanical properties. *International Journal of Molecular Sciences*, *20*. https://doi.org/10.3390/ijms20020371

Swimm, A., Bommarius, B., Li, Y., Cheng, D., Reeves, P., Sherman, M. et al. (2004) Enteropathogenic *Escherichia coli* use redundant tyrosine kinases to form actin pedestals. *Molecular Biology of the Cell*, *15*, 3520–3529. https://doi.org/10.1091/mbc.e04-02-0093

Tait, S.W. & Green, D.R. (2013) Mitochondrial regulation of cell death. *Cold Spring Harbor Perspectives in Biology*, *5*, a008706. https://doi.org/10.1101/cshperspect.a008706

Thanabalasuriar, A., Bergeron, J., Gillingham, A., Mimee, M., Thomassin, J.-L., Strynadka, N. et al. (2012) Sec24 interaction is essential for localization and virulence-associated function of the bacterial effector protein NleA. *Cellular Microbiology*, *14*, 1206–1218. https://doi.org/10.1111/j.1462-5822.2012.01789.x

Vingadassalom, D., Kazlauskas, A., Skehan, B., Cheng, H.-C., Magoun, L., Robbins, D. et al. (2009) Insulin receptor tyrosine kinase substrate links the *E. coli* O157:H7 actin assembly effectors Tir and EspFU during pedestal formation. *Proceedings of the National Academy of Sciences*, *106*, 6754–6759. https://doi.org/10.1073/pnas.0809131106

Vishnyakova, T.G., Bocharov, A.V., Baranova, I.N., Chen, Z., Remaley, A.T., Csako, G. et al. (2003) Binding and internalization of lipopolysaccharide by Cla-1, a human orthologue of rodent scavenger receptor B1. *Journal of Biological Chemistry*, *278*, 22771–22780. https://doi.org/10.1074/jbc.M211032200

Walle, L.V. & Lamkanfi, M. (2016) Pyroptosis. *Current Biology*, *26*, R568–R572. https://doi.org/10.1016/j.cub.2016.02.019

Weiss, S.M., Ladwein, M., Schmidt, D., Ehinger, J., Lommel, S., Städing, K. et al. (2009) IRSp53 links the enterohemorrhagic *E. coli* effectors Tir and EspFU for actin pedestal formation. *Cell Host and Microbe*, *5*, 244–258. https://doi.org/10.1016/j.chom.2009.02.003

Zanou, N., Mondin, L., Fuster, C., Seghers, F., Dufour, I., de Clippele, M. et al. (2015) Osmosensation in TRPV2 dominant negative expressing skeletal muscle fibres. *Journal of Physiology*, *593*, 3849–3863. https://doi.org/10.1113/JP270522

Zhao, H., Pykäläinen, A. & Lappalainen, P. (2011) I-BAR domain proteins: linking actin and plasma membrane dynamics. *Current Opinion in Cell Biology*, *23*, 14–21. https://doi.org/10.1016/j.ceb.2010.10.005

Zhong, Q., Roumeliotis, T.I., Kozik, Z., Cepeda-Molero, M., Fernández, L.Á., Shenoy, A.R. et al. (2020) Clustering of Tir during enteropathogenic *E. coli* infection triggers calcium influx–dependent pyroptosis in intestinal epithelial cells. *PLoS Biology*, *18*, e3000986. https://doi.org/10.1371/journal.pbio.3000986

Zhou, R., Yazdi, A.S., Menu, P. & Tschopp, J. (2011) A role for mitochondria in NLRP3 inflammasome activation. *Nature*, *469*, 221–226. https://doi.org/10.1038/nature09663

SUPPORTING INFORMATION

Additional supporting information may be found in the online version of the article at the publisher's website.

How to cite this article: Zhong, Q., Chatterjee, S., Choudhary, J.S. & Frankel, G. (2022) EPEC-induced activation of the Ca^{2+} transporter TRPV2 leads to pyroptotic cell death. *Molecular Microbiology*, 117, 480–492. https://doi.org/10.1111/mmi.14863